JOURNAL OF VIROLOGY, Aug. 2009, p. 7507–7516 Vol. 83, No. 15
0022-538X/09/$08.00+0 doi:10.1128/JVI.00495-09

Coronavirus Genetically Redirected to the Epidermal Growth Factor Receptor Exhibits Effective Antitumor Activity against a Malignant Glioblastoma▽

Monique H. Verheije,[1] Martine L. M. Lamfers,[2] Thomas Würdinger,[1]† Guy C. M. Grinwis,[3] Winald R. Gerritsen,[4] Victor W. van Beusechem,[4] and Peter J. M. Rottier[1]*

Virology Division, Department of Infectious Diseases and Immunology, Utrecht University, Utrecht, The Netherlands[1]; Department of Neurosurgery, Erasmus University, Rotterdam, The Netherlands[2]; Pathology Division, Department of Pathobiology, Utrecht University, Utrecht, The Netherlands[3]; and Department of Medical Oncology, VU University Medical Center, Amsterdam, The Netherlands[4]

Received 10 March 2009/Accepted 6 May 2009

Coronaviruses are positive-strand RNA viruses with features attractive for oncolytic therapy. To investigate this potential, we redirected the coronavirus murine hepatitis virus (MHV), which is normally unable to infect human cells, to human tumor cells by using a soluble receptor (soR)-based expression construct fused to an epidermal growth factor (EGF) receptor targeting moiety. Addition of this adapter protein to MHV allowed infection of otherwise nonsusceptible, EGF receptor (EGFR)-expressing cell cultures. We introduced the sequence encoding the adaptor protein soR-EGF into the MHV genome to generate a self-targeted virus capable of multiround infection. The resulting recombinant MHV was viable and had indeed acquired the ability to infect all glioblastoma cell lines tested in vitro. Infection of malignant human glioblastoma U87ΔEGFR cells gave rise to release of progeny virus and efficient cell killing in vitro. To investigate the oncolytic capacity of the virus in vivo, we used an orthotopic U87ΔEGFR xenograft mouse model. Treatment of mice bearing a lethal intracranial U87ΔEGFR tumor by injection with MHVsoR-EGF significantly prolonged survival compared to phosphate-buffered saline-treated ($P = 0.001$) and control virus-treated ($P = 0.004$) animals, and no recurrent tumor load was observed. However, some adverse effects were seen in normal mouse brain tissues that were likely caused by the natural murine tropism of MHV. This is the first demonstration of oncolytic activity of a coronavirus in vivo. It suggests that nonhuman coronaviruses may be attractive new therapeutic agents against human tumors.

Already for quite some years oncolytic viruses are being investigated for use in human tumor therapy (for recent reviews, see references 3, 16, 22, 37, and 44). Their success in destroying human cancer cells depends on their ability to selectively infect and kill these cells. Although some oncolytic viruses appear to have a natural tropism for tumor cells, most viruses need to be modified in some way to achieve infection and/or lytic activity in these cells. One of the ways to accomplish specific infection of tumor cells is by redirecting the virus to epitopes expressed on such cells. Thus, different targeting approaches have been explored for a variety of viruses. These include pseudotyping, modification of viral surface proteins, and the use of bispecific adapters (14, 35, 45). All of these approaches require that the viability of the virus is not hampered and that the targeting moiety is properly exposed to allow directed infection. The ability to genetically modify a particular virus combined with the availability of an appropriate targeting epitope determines the success of the approaches.

Coronaviruses are enveloped, positive-strand RNA viruses belonging to the order *Nidovirales.* The nonhuman coronavirus murine hepatitis virus (MHV) is the best-studied coronavirus and, more importantly, convenient reverse genetics systems are available to modify its genome (19, 50). MHV has several appealing characteristics that might make it suitable as an oncolytic virus. First, it has a narrow host range, determined by the interaction of its spike (S) glycoprotein with the cellular receptor mCEACAM1a. Since mCEACAM1a is not expressed on human cells, MHV cannot establish an infection in either normal or cancerous human cells. Second, infection by MHV induces the formation of large multinucleated syncytia, to which also surrounding uninfected cells are recruited (42). Hence, given also its relatively short replication cycle (6 to 9 h), MHV destroys populations of cells rapidly once they have become infected. Third, the tropism of MHV can be modified either by substitution of the viral spike ectodomain (19) or by the use of adapter proteins (43, 47, 48). These adapter proteins, composed of a virus-binding moiety coupled to a target cell-binding device, can redirect the virus to a specific receptor on the target cell (43, 47, 48). The studies revealed that, once the host cell tropism barrier is alleviated, MHV is capable of establishing infection in nonmurine cells.

The use of adapter proteins to target therapeutic viruses to tumor cells (modeled in Fig. 1A) is limited by the necessity to externally provide and replenish the adapter protein. To overcome this obstacle, the genetic information for the targeting device can be introduced into the viral genome to allow the virus to produce the adaptor itself in infected cells, thereby

* Corresponding author. Mailing address: Virology Division, Department of Infectious Diseases and Immunology, Utrecht University, Yalelaan 1, 3584 CL Utrecht, The Netherlands. Phone: 31 30 253 2462. Fax: 31 30 253 6723. E-mail: p.rottier@uu.nl.

† Present address: Departments of Neurology and Radiology, Harvard Medical School, Boston, Massachusetts, and Neuro-oncology Research Group, Department of Neurosurgery, VU Medical Center, Cancer Center Amsterdam, Amsterdam, The Netherlands.

▽ Published ahead of print on 13 May 2009.

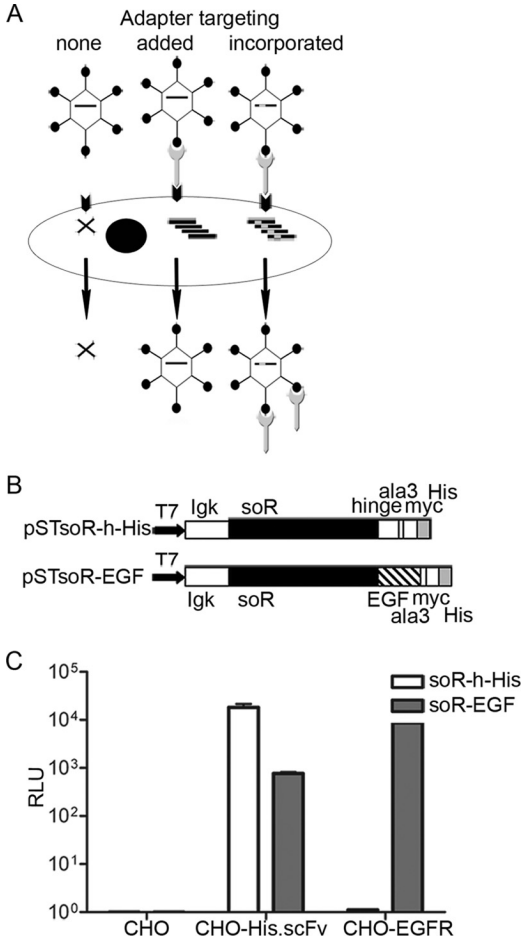

FIG. 1. Redirection of MHV to the EGFR. (A) Rationale for using adapter proteins to target viruses to a specific receptor present on target cells. Adapters, either added or expressed from the viral genome when incorporated, enable targeted infection of otherwise nonsusceptible cells. (B) Schematic diagram of the expression constructs pSTsoR-h-His and pSTsoR-EGF. The Igκ signal sequence directs adapter protein secretion, the N-terminal D1 domain of mCEACAM1a (soR) provides for binding to and induction of conformational changes in the MHV spike protein, and the six-amino-acid His tag (His) provides for binding to the artificial His receptor. The hinge (h) linker region present in soR-h-His allows formation of disulfide-linked dimers of the resulting adapter protein (43) (T7, T7 promoter; myc, myc tag; ala3, alanine tripeptide). (C) Targeting of MHV-EFLM to the His receptor and to the EGFR on CHO cells using soR-h-His and soR-EGF, respectively. CHO, CHO-His.scFv, and CHO-EGFR cells were inoculated with MHV-EFLM preincubated with soR-h-His or soR-EGF, and the luciferase activities (expressed as relative light units [RLU]) were measured. The values depicted are the means of an experiment performed in triplicate. Error indicators show the standard deviations.

creating a self-targeted virus. Indeed, we demonstrated the feasibility of this concept by expressing an adapter protein—composed of the relevant (soluble) domain of the mCEACAM1a receptor linked to a His tag—as an additional protein from the MHV genome (43). We extend these investigations here by coupling the epidermal growth factor (EGF) protein to the mCEACAM1a fragment. Introduction of this expression cassette encoding the adapter protein allowed multiround infection in EGF receptor (EGFR)-expressing human cells, resulting in extensive cell-cell fusion and efficient killing of target human glioblastoma cells. Using an orthotopic intracranial tumor model of aggressive U87ΔEGFR glioblastomas in nude mice, we show for the first time that redirected coronavirus has oncolytic potential.

MATERIALS AND METHODS

Cells and viruses. Murine LR7 cells (19); feline FCWF-4 cells (34); murine Ost-7 cells (13), hamster CHO, CHO-His.scFv (18), and CHO-EGFR cells (the latter two kindly provided by T. Nakamura, Rochester, MN [29]); and human glioblastoma U373MG, U251MG, Gli6MG, U87MG, and U87ΔEGFR cells (the generation of U87ΔEGFR is described in reference 31) were all maintained in Dulbecco modified Eagle medium (Cambrex BioScience, Verviers, Belgium) containing 10% fetal calf serum, 100 IU of penicillin/ml, and 100 μg of streptomycin/ml (all from Life Technologies, Ltd., Paisley, United Kingdom).

Stocks of MHV-EFLM (8), MHVd2aHE (7), recombinant felinized fMHV (19), and MHVsoR-h-His (43) were grown and titrated as described previously (43).

Construction of the genes encoding the adapter proteins soR-h-His and soR-EGF and production of the adapter proteins. The construction of soR-h-His has been described elsewhere (43). The gene encoding the amino-terminal D1 domain of the mCEACAM1a receptor (soR) fused to EGF was generated similarly. Briefly, to generate the EGF gene, two annealing primers were used as a template in a PCR (CATTGCGGCCGCCAATAGTGACTCTGAATGTCCCCTG TCCCACGATGGGTACTGCCTCCATGATGGTGTGTGCATGTATATTG AAGCTCTAGACAAGTAT, sense, nucleotides [nt] 1 to 90; and ACTTGGGC CCGCGCAGTTCCCACCACTTCAGGTCTCGGTACTGACATCGCTCCCC GATGTAGCCAACAACACAGTTGCATGCATACTTGTCTAGAGCTTC, antisense, nt 70 to 160) using a forward primer (TGCAGCGGCCGCCAATAG TGACTCTGAATGT, sense, nt 1 to 18) and a reverse primer (CTAGGCGGC CGCGCGCAGTTCCCACCACTT, antisense, nt 141 to 159). The resulting DNA fragment contained a 5′ and 3′ NotI site (underlined in the primers) and was subsequently cloned using this restriction enzyme into pSTsoR-His (43), a derivative of the expression vector pSecTag2 (Invitrogen, Breda, The Netherlands), resulting in pSTsoR-EGF. The sequence of the gene encoding the adapter protein was confirmed by sequencing. Recombinant vaccinia virus vTF7-3 expressing the bacteriophage T7 RNA polymerase gene was used as a T7 RNA polymerase source for T7 promoter-driven production of the soR adapter proteins in OST7-1 cells (10) as described previously (43).

Luciferase expression assay. Monolayers of 0.32 cm^2 of CHO, CHO-His.scFv, and CHO-EGFR cells were inoculated with 10^4 tissue culture infective doses ($TCID_{50}$; as determined by endpoint dilution on LR7 cells) of the firefly luciferase-expressing MHV-EFLM (8) preincubated at 4°C for 1 h with the indicated amounts of adapter proteins. At the indicated time points, the cells were lysed, and intracellular luciferase expression was measured as described previously (43).

Targeted RNA recombination. The construction of MHVsoR-h-His by targeted RNA recombination has been described before (43). MHVsoR-EGF was generated in a similar way; first, a transcription regulation sequence (TRS) was introduced into pSTsoR-EGF directly upstream of the soR-encoding region to allow expression of the adapter proteins from an additional expression cassette in the MHV-A59 genome. Next, the fragment TRS-soR-EGF was cloned in two successive steps into pMH54 (19), resulting in transcription vector pMHsoR-EGF suitable for targeted recombination. Targeted RNA recombination was performed as described previously (7, 19). Briefly, donor RNA transcribed in vitro from the PacI-linearized plasmid pMHsoR-EGF was transfected by electroporation into feline FCWF-4 cells that had been inoculated at a multiplicity of infection (MOI) of 0.5 with fMHV 4 h earlier. These cells were then plated in culture flasks, and the culture supernatant was harvested 24 h later. Progeny virus was plaque purified, and virus stocks were grown in LR7 cells. After confirmation of the presence of the additional expression cassette by reverse transcription-PCR on purified viral RNA from these virus stocks, the titers of the stocks were determined by endpoint dilution on LR7 cells. These passage 2 virus stocks were subsequently used in the experiments.

Analysis of viral growth kinetics. An amount of 10^5 cells per 2-cm^2 well of the indicated cells was inoculated with 0.5×10^5 $TCID_{50}$. After 1 h, the culture supernatant was removed, the cells were washed, and fresh culture medium was added. At several time points postinfection (p.i.), an 20-μl aliquot of the medium was harvested and stored at −80°C until analysis. The amount of virus produced at each time point was determined by endpoint dilution on LR7 cells, and the $TCID_{50}$ values were calculated.

Antibody blocking experiments. To determine whether MHVsoR-EGF infection of CHO-EGFR cells is specifically mediated by the EGFR, cells were preincubated with different amounts of hybridoma supernatant containing monoclonal antibody (MAb) 425 directed against the EGFR for 30 min at 4°C. Next, the cells were inoculated with 10^4 $TCID_{50}$ of MHVsoR-EGF for 1 h at 37°C. The cells were washed and incubated for 20 h, after which they were fixed and stained to analyze the expression of viral proteins.

Immunoperoxidase staining of cell cultures. Cells inoculated with MHVsoR-h-His or MHVsoR-EGF were fixed with phosphate-buffered saline (PBS) containing 3.7% paraformaldehyde. Immunostainings were performed as described before (43) using K135 anti-MHV serum (36).

Monolayer cytotoxicity analysis. A total of 5×10^4 U87ΔEGFR cells per 0.32-cm^2 well was seeded and infected the next day in triplicate with MHVsoR-EGF at an MOI of 5. At several time points after inoculation, the culture medium was replaced by Dulbecco modified Eagle medium containing 10% WST-1 (Roche Diagnostics GmbH, Mannheim, Germany), and the cells were cultured for 30 min. Hereafter, the optical density at 450 nm was measured, and the viability of the infected cells was determined as described previously (43).

Animal experiments. For assessing the therapeutic effect of MHVsoR-EGF in vivo, an intracranial glioblastoma xenograft mouse model was applied as described previously (20). Eight-week-old female SPF athymic *nu*/*nu* mice (Harlan, Horst, The Netherlands) were stereotactically injected with 10^5 U87ΔEGFR cells in 3 μl of PBS into the right frontal lobe, 2.5 mm lateral to the bregma at a depth of 2.5 mm. Injections were done under anesthesia induced by intraperitoneal injection of 2 mg of ketamine and 0.4 mg of xylazine in 0.9% saline. After 4 days, 10^5 MHVsoR-EGF, 10^5 MHVsoR-h-His, or PBS, all in a total volume of 3 μl, was inoculated stereotactically into the same coordinates. Animals were monitored daily and sacrificed upon manifestation of clinical symptoms, such as paralysis and lethargy, indicative of a moribund state. From each experimental group, one animal was sacrificed at day 9 after tumor cell inoculation, while the others were monitored long term to be able to score for survival (MHVsoR-h-His and PBS treated [each group composed of eight mice] and MHVsoR-EGF treated [seven mice; one animal in this group died preliminarily due to an unrelated cause]). Brains were removed and preserved in 4% neutral-buffered formaldehyde for histological analyses. Animal experiments were approved by the local committee on animal experiments and carried out in compliance with Dutch laws.

Histopathology and immunohistochemistry. The brains were fixed in 4% neutral-buffered formaldehyde overnight and subsequently trimmed and paraffin embedded. Brain samples that included the area of inoculation were cut into 4-μm sections by using a standard microtome (sectioned from cranial to caudal). Hematoxylin-eosin staining was performed on tissue sections to analyze morphology and the presence of neoplastic cells by light microscopy. Staining for viral proteins (on seven of seven brains from the MHVsoR-EGF-treated group and on three of eight brains from the MHVsoR-h-His-treated group) was performed as described by de Haan et al. (6).

Statistical analysis. For mice with intracerebral tumors, statistically significant differences in survival between treatment group and control groups were assessed by the Wilcoxon test.

RESULTS

Generation of EGFR-directed adapter proteins and their ability to redirect MHV to the EGFR. The EGFR is currently considered a very suitable target for virotherapy due to its high abundance on most tumors. Thus, we designed an adapter protein composed of the 53-amino-acid EGF protein linked directly to the N-terminal D1 domain of the MHV receptor mCEACAM1a (soR) to which we added a C-terminal myc and His tag. A schematic picture of the construct is depicted in Fig. 1B, along with the control construct lacking the EGF gene which was optimized for targeting to an artificial His receptor (43).

Both adapter proteins were produced by using a vaccinia virus T7 expression system in Ost-7 cells. Western blot analysis of the culture supernatants using antibodies raised against N-CEACAM-Fc (15) showed that the adapter proteins were properly synthesized and secreted (data not shown).

To study the targeting capacities of the soR-EGF adapter protein, we selected three CHO cell lines: wild-type cells, which are refractory to MHV infection and without detectable EGFR expression; CHO-His.scFv cells constitutively expressing an artificial His receptor (i.e., a membrane-anchored, single-chain antibody that recognizes a six-histidine peptide [18]) and CHO-EGFR cells expressing the wild-type EGFR (29). MHV-EFLM, an MHV (strain A59) derivative expressing firefly luciferase (8), was incubated with equal amounts of the adapter proteins (as determined by Western bloting) and subsequently inoculated onto the wild-type or mutant CHO cells. Luciferase activity was measured to determine whether inoculation had resulted in successful infection of the target cells (Fig. 1C). The data show that whereas both soR-EGF and soR-h-His were able to redirect MHV-EFLM to the CHO-His.scFv cells, infection of CHO-EGFR cells could only be achieved by preincubating the virus with soR-EGF and not with the soR-h-His protein. This result demonstrated that the infection of CHO-EFGR cells was mediated specifically by the EGF targeting moiety present in the soR-EGF adapter protein. Similar inoculations of the parental CHO cell line resulted in background levels of luciferase activity only, both with soR-h-His and with soR-EGF.

Generation and growth characteristics of recombinant MHVsoR-h-His and MHVsoR-EGF viruses. Our next aim was to incorporate the adapter genes into the viral genome in order to generate viruses that produce their own targeting devices, thereby acquiring the ability to independently multiply in the appropriate target cells. Thus, recombinant viruses MHVsoR-h-His (described elsewhere [43]) and MHVsoR-EGF, both derivatives of MHV strain A59, in which the adapter genes replace the viral genes 2a/HE, were produced by using targeted RNA recombination technology (Fig. 2A). These viruses replicated in murine LR7 cells with similar kinetics and to approximately similar titers as MHVd2aHE, a virus lacking the 2a/HE genes (Fig. 2B). They were found to stably maintain their inserts for at least five passages (data not shown).

MHVsoR-EGF can specifically infect EGFR-expressing cells. To demonstrate that the adapter protein soR-EGF was produced from the expression cassette in the recombinant MHVsoR-EGF viruses, CHO-EGFR cells were inoculated with the recombinant MHV viruses, incubated for 20 h, and processed for an immunoperoxidase labeling using anti-MHV serum. Microscopic analysis of the cells showed staining of viral proteins in cultures inoculated with MHVsoR-EGF but not in those inoculated with MHVsoR-h-His (Fig. 3A). Large areas of cell-cell fusion were observed in the MHVsoR-EGF-infected CHO-EGFR cells, a finding indicative of an intact fusion capacity of the virus when expressing a soR-EGF adapter (Fig. 3A; shown at ×20 magnification). Inoculation of wild-type CHO cells did not result in the expression of viral proteins, indicating that EGFR-negative cells could not be infected with this virus. The specificity of the targeted infection was confirmed by showing that the virus could be blocked in a dose-dependent manner by an MAb directed against the EGFR (Fig. 3B). The infection could not be fully blocked by this MAb, which was likely due to the rather low concentration of this MAb in the culture supernatant of the hybridoma cell line from which it was obtained.

Analysis of the characteristics of MHVsoR-EGF recombinant virus in human glioblastoma cells. To determine whether

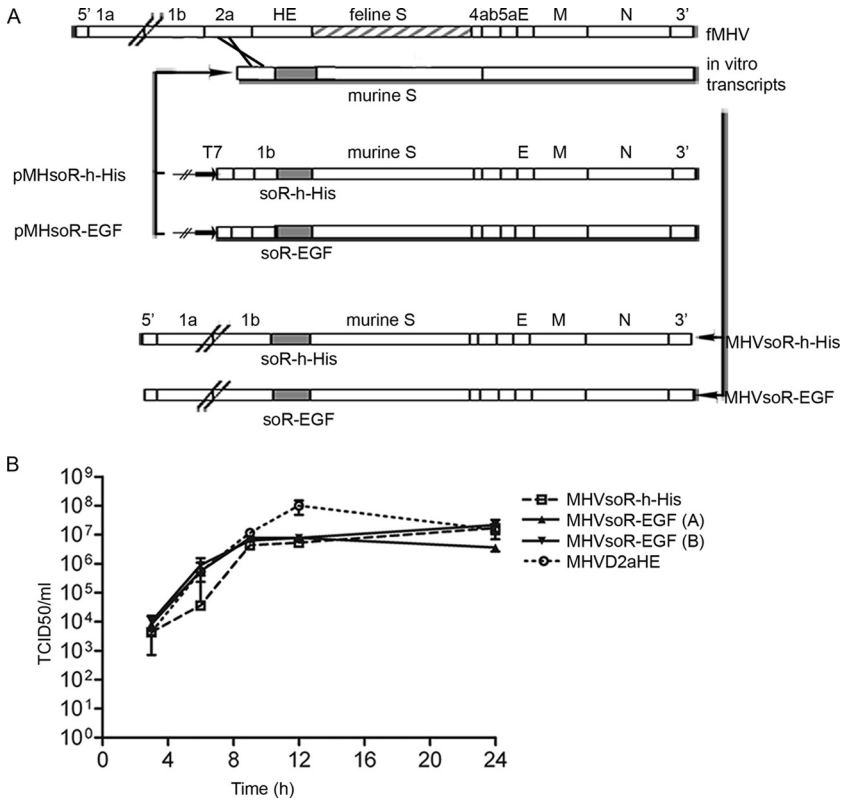

FIG. 2. Recombinant MHVsoR-h-His and MHVsoR-EGF viruses and their growth kinetics in murine cells. (A) Targeted recombination: principle, vectors, and recombinant viruses. At the top, the principle of the method is depicted showing the recombination between the recipient fMHV and the donor in vitro RNA transcript. The transcription vectors from which the RNAs are transcribed in vitro by T7 RNA replicase are depicted in the middle. The inserted additional expression cassettes encoding soR-h-His and soR-EGF are represented by a grey box. The recombinant virus genomes generated by targeted RNA recombination are depicted below. (B) Growth kinetics of the MHV recombinants in LR7 cells. LR7 cells were infected at an MOI of 0.5, the production of progeny virus in the culture supernatant at different times p.i. was determined by endpoint dilution on LR7 cells, and the $TCID_{50}$ values were calculated. Panels A and B indicate independently generated recombinants.

the soR-EGF-expressing recombinant MHV is able to infect human tumor cells displaying the EGFR, we selected several human glioblastoma cell lines, each one expressing the EGFR endogenously (28), and the U87ΔEGFR cell line additionally expressing a mutant EGFR gene with a deletion of exon 2-7, which is a common deletion in glioblastoma tumors (31). The U373MG, U251MG, Gli6MG, U87MG, and U87ΔEGFR cells were each inoculated in parallel with MHVsoR-h-His and with MHVsoR-EGF, fixed at 18 h postinoculation, and processed for an immunoperoxidase labeling using anti-MHV serum. Microscopic analysis of the cells showed staining of viral proteins in all tumor cell cultures inoculated with MHVsoR-EGF but not in cells inoculated with MHVsoR-h-His virus (Fig. 4A). No striking differences in the number of infected cells were observed between the different cell lines except for the U251MG cell line, which displayed somewhat less infection. This reduced level of infection did not correspond to a relatively lower level of the EGFR in these cells (data not shown). Furthermore, all glioblastoma cell lines showed syncytium formation, a finding indicative of the retained fusion capacity of the MHV spike protein.

To analyze whether MHVsoR-EGF could establish a multiround infection of the target cells, we inoculated 5×10^4 glioblastoma cells with 10^5 $TCID_{50}$ units of MHVsoR-EGF (as titrated on LR7 cells; the infectivity of MHV for glioblastoma cells was 100- to 1,000-fold lower than for LR7 cells as observed by comparative immunostaining on all cell lines [data not shown]). Cell viability was measured by WST-1 assay at different time points after inoculation (Fig. 4B). Our results showed that MHVsoR-EGF spreads through the U87ΔEGFR cell cultures, killing increasing numbers of cells and eventually eradicating the entire culture. Surprisingly, the EGFR-redirected MHV did not affect the viability of the U373MG, U251MG, Gli6MG, and U87MG cell lines, suggesting that other intrinsic factors in the tumor cells play a role in the ability of this virus to kill these cell cultures. As expected, MHVsoR-h-His did not affect the viability of U87ΔEGFR cell cultures.

To confirm that the observed killing of U87ΔEGFR cells by MHVsoR-EGF was due to the production and spread of progeny virus, we prepared an in vitro growth curve of the virus in these cells, as described in Materials and Methods. Figure 4C demonstrates that recombinant MHVsoR-EGF virus replicated with normal kinetics and with quite normal yields, reaching maximal titers of 10^6 to 10^7 $TCID_{50}$/ml, as determined by endpoint dilution on LR7 cells. In contrast, inoculation of U87ΔEGFR cells with the control virus MHVsoR-h-His did not, as expected, give rise to progeny virus production.

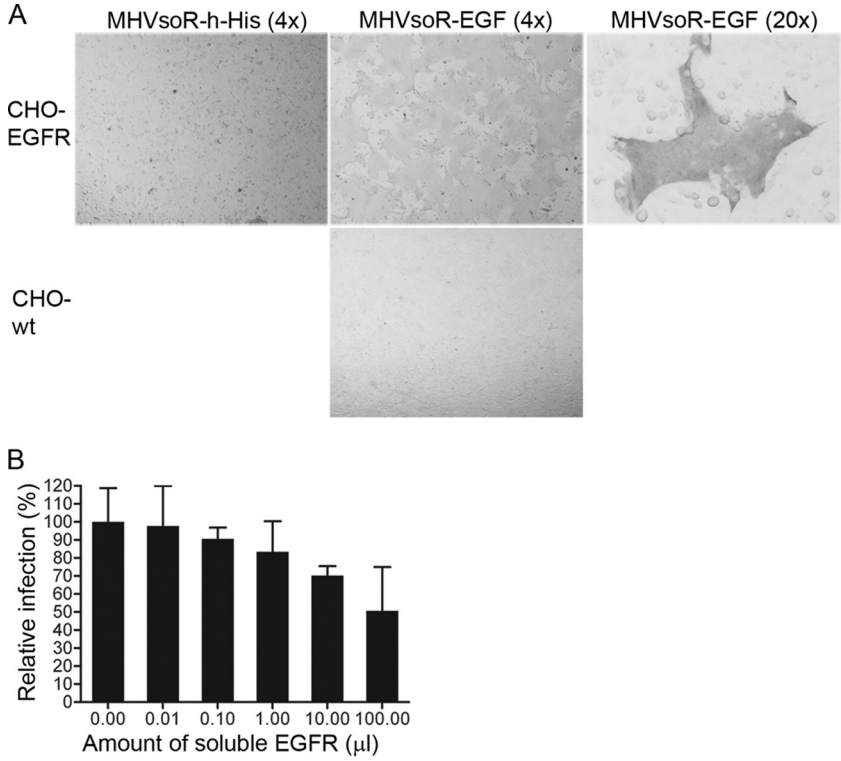

FIG. 3. Receptor specificity of MHVsoR-EGF recombinant virus. (A) Immunoperoxidase staining of CHO-EGFR and CHO-wt cells inoculated with MHVsoR-h-His and MHVsoR-EGF recombinant viruses using anti-MHV serum K135. Images are shown at ×4 magnification, and images for the recombinant MHVsoR-EGF virus syncytium formation are also shown at ×20 magnification. (B) MHVsoR-EGF was inoculated onto CHO-EGFR cells preincubated for 1 h at 4°C in the absence or presence of increasing amounts of anti-EGFR MAb 425. At 20 h p.i., the cells were fixed, permeabilized, and stained for MHV protein expression using anti-MHV serum K135. The number of stained cells was counted and is depicted relative to the number of positive cells counted in the control culture preincubated in the absence of MAb 425. The data represent the relative number of infected cells compared to mock-treated cells. Error bars show the standard deviations of experiments performed in triplicate.

In conclusion, the EGFR retargeted MHVsoR-EGF, but not the control virus MHVsoR-h-His, is able to establish infection and produce progeny virus, with subsequent killing of the human glioblastoma U87ΔEGFR cells in vitro.

In vivo efficacy studies. U87ΔEGFR cells are known to have a high tumorigenic capacity in vivo (31). Thus, we decided to evaluate the oncolytic capacity of the redirected virus in an established intracranial U87ΔEGFR glioblastoma model in vivo. In this model, tumor growth is aggressive, often leading to the appearance of neurological symptoms (such as hemiparesis and behavioral changes) and ultimately to a moribund decline and death of mice ~21 days after tumor cell injection. Tumors were established by injection of 10^5 U87ΔEGFR cells in the right hemisphere of the mouse brains as described previously (20). Four days later, mice were injected intracranially at the same coordinates with either 10^5 $TCID_{50}$ MHVsoR-EGF, 10^5 $TCID_{50}$ MHVsoR-h-His, or PBS. From each group one animal was sacrificed at day 9 after tumor cell injection (i.e., day 5 after treatment) to analyze initial tumor development in the acute phase of the infection. The remaining animals in each group were monitored daily and sacrificed when obvious neurological symptoms appeared or when a weight loss exceeding 20% of the original weight was observed.

Treatment with MHVsoR-EGF had a dramatic effect on survival (Fig. 5). Survival times of the animals were significantly extended compared to both MHVsoR-h-His- and PBS-treated mice ($P = 0.004$ and $P = 0.001$, respectively). No significant difference between survival of PBS- and control virus-treated mice was observed ($P = 0.33$). The observed median survival times were 16, 19.5, and 41 days for PBS-, control virus-, and redirected virus-treated mice, respectively. Histopathological analysis of hematoxylin-eosin-stained sections of the brains removed from animals killed at day 9 after glioblastoma cell injection revealed the presence of neoplasms in the brains of the PBS- and MHVsoR-h-His treated mice, whereas in the brain of the MHVsoR-EGF treated mouse no neoplasm could be observed (shown in Fig. 6A, Day 9). Serial sections of all brains showed significant cyst formation in the area of injection. These cysts were optically largely empty, showing some extravasated erythrocytes and various numbers of macrophages with lipofuscin, hemosiderin pigment, and neutrophils. It is of note that no clinical symptoms were observed in any of the mice at this time point in the study (Day 9).

At the onset of significant neurological symptoms (e.g., paralysis) and/or weight loss, animals were sacrificed. Histopathological analysis of the brains of sacrificed mice (indicated, Day > 9 in Fig. 6A revealed large neoplasms in all brains inoculated with PBS and in six of seven analyzed brains of mice treated with the control virus. In contrast, no tumor load could be detected in the brains of six of seven mice treated

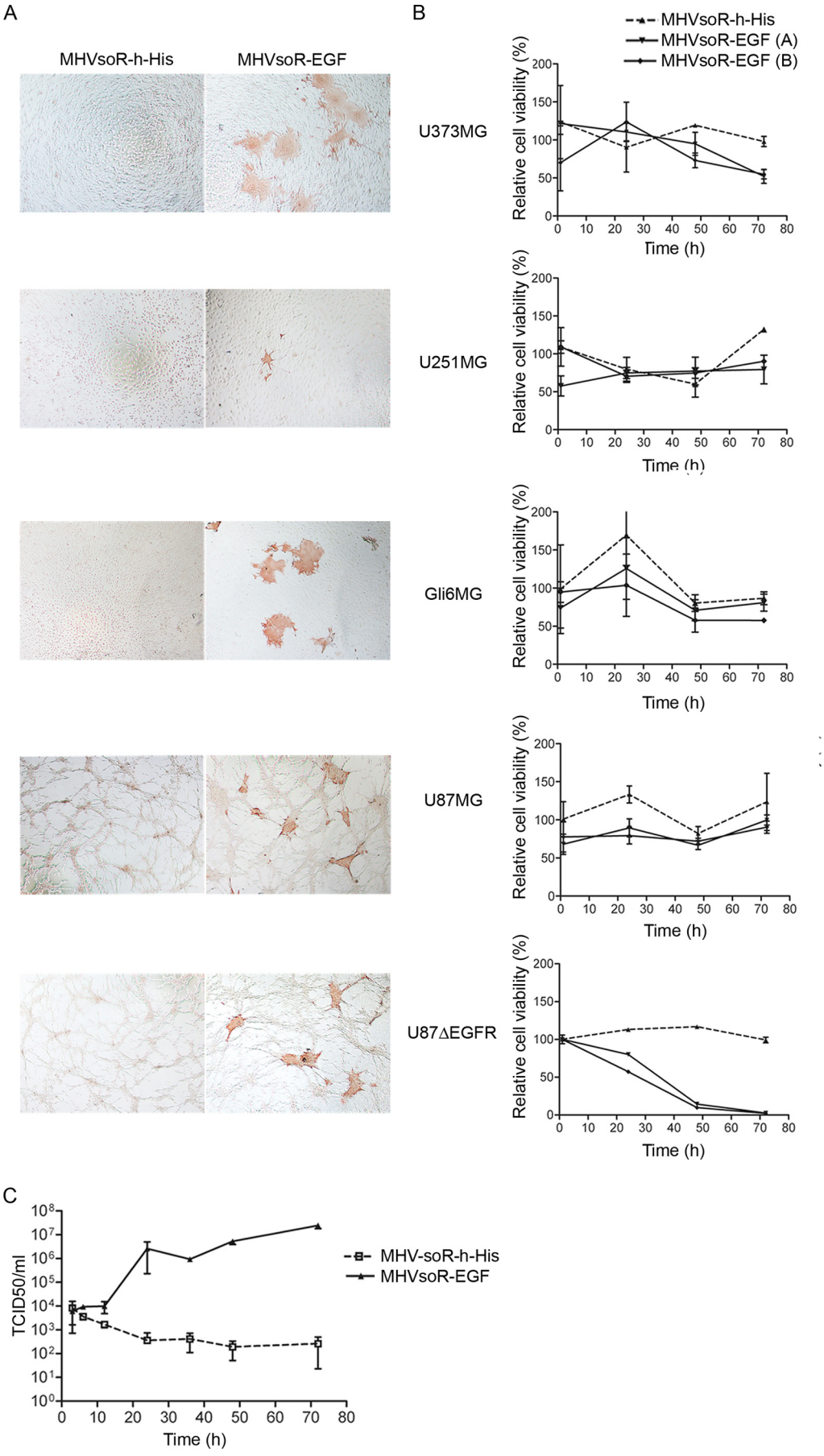

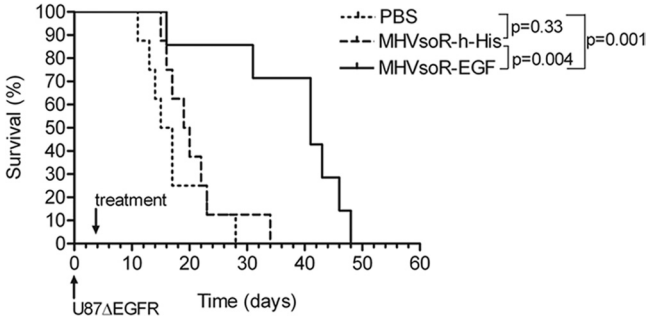

FIG. 5. In vivo oncolytic activity of MHVsoR-EGF. Mice with established intracranial U87ΔEGFR tumors were treated with MHVsoR-EGF, MHVsoR-h-His or PBS at 4 days after tumor cell inoculation. The animals were monitored, and mice with obvious neurological symptoms or weight loss exceeding 20% of the original weight were euthanized. The Kaplan-Meier curves showing survival of mice are depicted.

with the retargeted MHVsoR-EGF (a representative example is shown in Fig. 6A, Day > 9). The animal treated with the control virus in which no neoplasm could be detected survived the longest in this group (34 days).

Immunohistochemical staining of sections with virus-specific polyclonal antiserum, counterstained with hematoxylin-eosin, showed viral protein expression in nonneoplastic tissue of the brains of MHVsoR-EGF- and MHVsoR-h-His-injected mice at day 9. At the time of sacrifice due to severe symptoms, five of seven analyzed MHVsoR-EGF-treated brains showed MHV-specific staining in nonneoplastic tissue (an example of an MHVsoR-EGF-treated brain obtained at day 43 is shown in Fig. 6B). Relative levels of infection of neoplastic and nonneoplastic tissue could not be determined in these brains, since no neoplastic tissue was present in any of these cases. One of the brains that could not be stained with MHV antibodies was of the single animal in which a tumor was observed at $t > 9$ days after injection with MHV-soR-EGF. In two of three analyzed control virus-treated mice, staining was observed, whereas no staining was observed in PBS-inoculated brains.

Despite the lack of neoplasms in six of seven mice treated with MHVsoR-EGF, these mice suffered from neurological symptoms, with ultimate moribund decline. Histopathological analyses of the brains revealed cystic structures with similar morphology as noted in animals killed after 9 days in five of six neoplasm-free animals treated with MHVsoR-EGF and also in the one mouse treated with MHVsoR-h-His without a neoplasm that was killed at a later stage of the experiment.

DISCUSSION

Despite great efforts, the treatment options for patients with malignant brain tumors are still very limited. Due to their often widely ramified nature and their anatomical location, complete surgical resection of these tumors is often not feasible. Hence, creative, minimally invasive new strategies are required among which virotherapy seems, at least conceptually, the most straightforward approach. We continued here our explorations of the potential of a new candidate oncolytic virus in vivo. We demonstrate that the nonhuman coronavirus MHV can be redirected to the EGFR by using adapter proteins consisting of a soluble mCEACAM1a receptor arm fused to the EGF protein. Genetic incorporation of the adapter sequence in the viral genome was tolerated, and the virus retained its ability to induce cell-cell fusion and produce progeny virus. Moreover, this recombinant virus mediated efficient cell killing of the human glioblastoma cell line U87ΔEGFR. Most importantly, the redirected virus MHVsoR-EGF was effective in eradicating the highly aggressive U87ΔEGFR tumor in an orthotopic mouse model. To our knowledge, this is the first evidence demonstrating in an animal model that coronaviruses have potential as antitumor agents.

Recently, we showed that the species barrier of coronaviruses can be alleviated by using adapter proteins (43, 47, 48). These adapter proteins were constructed in such a way that either both arms encoded single chain antibody fragments (scFv; e.g., the bispecific scFvs directed against the feline spike protein and the EGFR [48]), both arms encoded "regular" genes (e.g., the soluble mCEACAM1a and the artificial His tag [43]), or a combination of the two (e.g., soluble mCEACAM1a fused to the scFv directed against EGFR [47]). It appeared that the incorporation of adapter proteins consisting of either one or two scFvs in the viral genome was not tolerated by MHV; viruses expressing the adapter gene could not be stably maintained (unpublished data). Fortunately, such viruses could be prepared and maintained when the adapter gene was composed of sequences encoding the soluble mCEACAM1a receptor linked to an artificial His tag (43) or to EGF (the manuscript). The recombinant MHVs grew with characteristics comparable to those of MHVd2aHE, a similar virus lacking the adapter genes. Most likely, it is the sequence composition of the scFvs rather than insert size constraints that resist stable maintenance in the viral genome, since the introduction of significantly larger sequences has been successfully achieved earlier (8).

The in vivo oncolytic activity of our redirected MHV against the highly aggressive brain tumor U87ΔEGFR (31) appeared to be fast and lasting. Soon after virus inoculation, most of the tumor was found to be destroyed, and no recurrent tumor was

FIG. 4. Infection, cell killing, and progeny virus production in MHVsoR-EGF inoculated human glioblastoma cell lines. (A) Immunoperoxidase staining of EGFR-expressing human glioblastoma U373MG, U251MG, Gi6MG, U87MG, and U87ΔEGFR cells inoculated with recombinant virus MHVsoR-h-His or MHVsoR-EGF using anti-MHV serum K135. (B) Cell viability of glioblastoma U373MG, U251MG, Gi6MG, U87MG, and U87ΔEGFR cell lines after inoculation with MHVsoR-h-His and MHVsoR-EGF. The cell viability was measured at different time points after inoculation and is depicted relative to uninfected control cells. (C) Growth kinetics of MHVsoR-h-His and MHVsoR-EGF in U87ΔEGFR cells. The production of progeny virus in the culture media at different times postinfection was determined by endpoint dilution on murine LR7 cells, and the $TCID_{50}$ values were calculated.

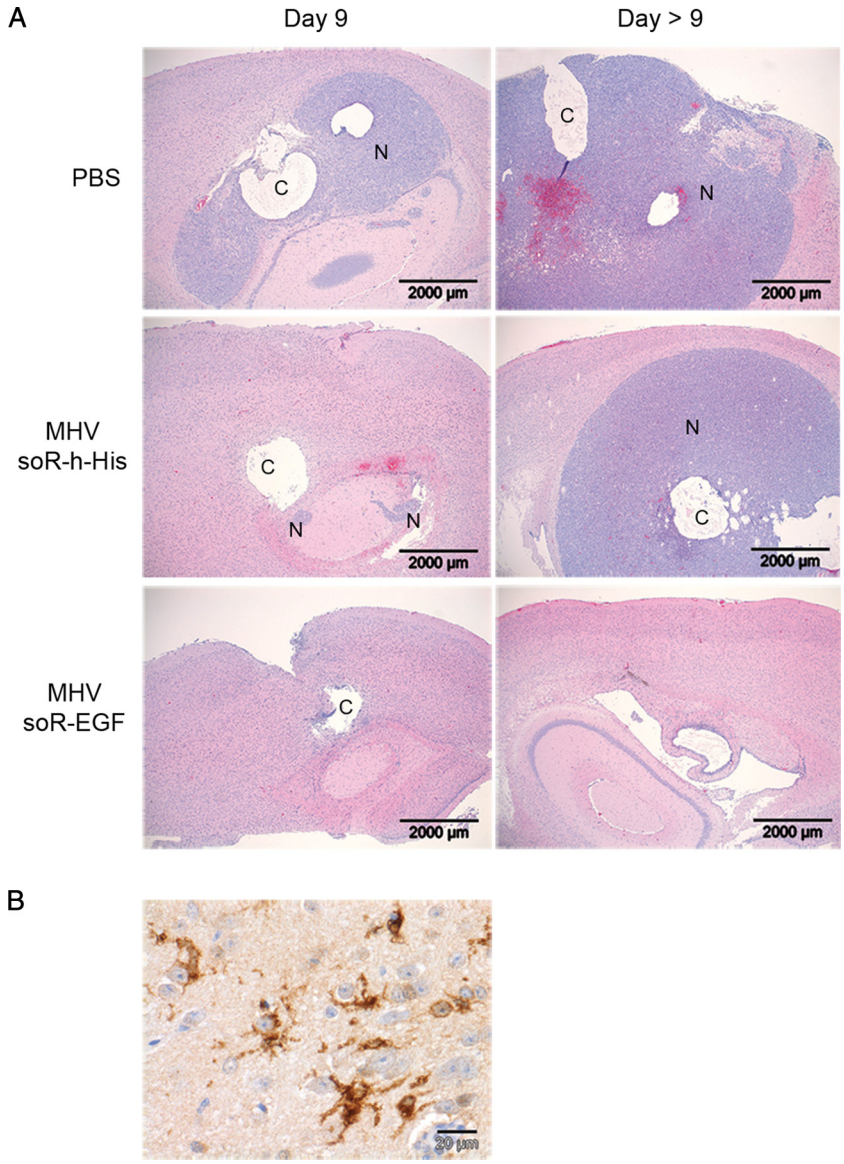

FIG. 6. Histopathological analysis of brains. (A) Representative hematoxylin-eosin stained slides of brains excised at 9 days (Day 9) or at a later day of euthanasia due to the occurrence of neurological symptoms (Day > 9) after establishing the U87ΔEGFR xenografts (for PBS-, control-, and targeted virus-treated mice days 17, 16, and 43 days after tumor cell injection, respectively). Large neoplasms and cystic structures are indicated by "N" and "C," respectively. (B) Immunohistochemical staining for viral proteins using polyclonal MHV antibody K135 and counterstained with hematoxylin. Shown is a section of the brain of an MHVsoR-EGF-treated U87ΔEGFR xenograft at the time of sacrifice (43 days after tumor cell injection). Note the appearance of immunoreactivity mainly in astrocytes and the absence of marked pathology.

observed in this orthotopic model in six of seven MHVsoR-EGF-treated animals. The single animal that had neoplastic tissue lacked any immunohistochemical staining for MHV, suggesting that the redirected virus had not been applied correctly. One other striking outlier was the animal in the control virus-treated group that survived the longest and in which no tumor tissue was observed, implying that this single U87ΔEGFR implantation had not been successful, since all other animals in this group developed large neoplasms.

One obvious drawback to studying the oncolytic capacity of MHV in a mouse model is the virus' natural tropism. It has been shown that MHV strain A59, the genetic background of our control and retargeted viruses, is weakly neurovirulent and causes demyelination in immunocompetent mice (38). However, no demyelination was observed in the brains of mice treated with the retargeted virus, since immunohistochemical staining with an antibody to the myelin basic protein appeared similar in infected and PBS control mouse brains (data not shown). Our recombinant MHV-A59 viruses lack the virulence gene cluster 2a/HE, a deletion that appeared to attenuate the virus as judged after intracranial inoculation in C57BI/6 mice (7). However, mouse tissue is likely to be still permissive to the recombinant viruses since they can be propagated in murine LR7 cells in vitro. Furthermore, our histopathological studies revealed cyst formation and secondary inflammatory changes. Moreover, we did observe substantial loss of tissue within the

injected area resulting in the formation of cysts with secondary local granulomatous and neutrophilic inflammation in both acute and later stages. The cysts most likely resulted from liquefactive necrosis of neoplastic tissue and not of necrosis of preexistent neural tissue. This is suggested by the absence of morphological indications of degeneration, necrosis, or inflammation in preexisting areas in the brain where MHV antigen was detected immunohistochemically. Liquefactive necrosis within the central nervous system typically results in cystic structures since the formation of granulation tissue, as is observed in other tissues during damage repair, does not occur in the central nervous system. In conclusion, the neurological symptoms recorded in the animals are probably related to growth of the neoplasms and/or formation of cystic structures in the brain tissue. Most likely, replication of the targeted MHV in nonneoplastic brain tissue caused the neurological symptoms observed in the mice treated with MHVsoR-EGF.

Several other viruses have been explored for their potential as oncolytic agents against glioblastomas. The first one genetically engineered and proven to be efficient in an experimental glioblastoma model was herpes simplex virus (27). Among the ones that followed were lentiviruses (40), vesicular stomatitis virus (24, 33), myxoma virus (25), measles virus (1), Newcastle disease virus (5, 12), and adenoviruses (reviewed in references 17 and 39). One major advantage of nonhuman coronaviruses is that they have a very short replication cycle, resulting in fast clearance of the tumor cells (already observed at day 5 postinoculation, Fig. 6). Their ability to cause cell-cell fusion of infected with noninfected neighboring cells is likely to contribute to this. Furthermore, MHV does not infect humans, so its natural tropism does not need to be ablated, nor will preexisting antibodies dampen its reproduction. The EGFR is an intriguing target in high-grade glioblastomas because it is often abundantly overexpressed (9, 21, 46). Moreover, the most frequently identified mutant EGFR in malignant glioblastomas is EGFRvIII, as is the case in U87ΔEGFR cells (11, 41, 49). EGFR is, however, also present to some extent on nonneoplastic tissue in the brain, indicating that improving the selectivity of targeting might be required.

Intriguingly, overcoming the entry barrier was not the only requirement for establishing a productive MHV infection. Although postentry blocks of viral replication have been described for several viruses (reviewed in reference 2), this has never been observed for MHV. Rather, the presence of the viral receptor mCEACAM1a thus far appeared to be the sole requirement for MHV multiplication. As we found out when inoculating several EGFR-expressing human glioblastoma cells with our self-targeted MHVsoR-EGF, successful infection including the induction of syncytium formation was achieved in all cases. Surprisingly, however, the infection did not spread and eradicate the culture except in one case, the U87ΔEGFR cells, which were efficiently killed by the virus. Although not studied here, it is unlikely that binding to the mutant EGFR (ΔEGFR or EGFRvIII) additionally expressed in the U87ΔEGFR cell line accounts for this difference since EGFRvIII is unable to bind EGF as a ligand (31), and EGFR levels are comparable for U87MG and U87ΔEGFR (31). Thus, although alleviation of the tropism barrier seems to be a prerequisite for MHV infection, its oncolytic properties might depend on other cellular signaling events, such as interferon signaling (as observed for poxvirus, vesicular stomatitis virus, and Newcastle disease virus), p53 (30), or Ras (4, 32). For instance, Ras activation mediates reovirus oncolysis by enhancing virus uncoating, particle infectivity, and apoptosis-dependent release (26). Moreover, it has been shown that EGFR overexpression or its aberrant functioning can lead to Ras activation (23). Hence, since U87ΔEGFR is constitutively active in EGFR signaling due to its deletion of exon 2-7, it will be of interest to investigate whether coronavirus replication is also affected by the Ras pathway.

The significant oncolytic activity of the new, redirected animal coronavirus observed in the present study seems to warrant further studies. In view of the complications associated with using a murine virus in a murine model, shifting to a relevant nonmouse model, such as immune deficient rats, seems the most logical option, since MHV does not replicate in other mammalian species. Such studies will hopefully allow us to establish oncolytic efficacy of the recombinant MHV in immunocompetent animals, as well as in other tumors.

ACKNOWLEDGMENTS

We thank T. Nakamura (Mayo Clinic College of Medicine) for providing the CHO cell lines; J. Brakkee (Rudolf Magnus Institute of Neuroscience) and S. Idema (VU University Medical Center) for lending us stereotactic frames; S. Moeniralm (VU University Medical Center), C. Bekker (Utrecht University), M. Raaben (Utrecht University), and H. J. Prins (UMC Utrecht), and the Animal Facility staff for help with animal experiments; and people from the Histology and Pathology Departments (Utrecht University) for performing the histological stainings.

This study was supported in part by Dutch Cancer Society project UU 2001-2430. M.H.V. was partly supported by a grant from the Hersenstichting Nederland, and V.W.V.B. was supported by a research fellowship from the Royal Netherlands Academy of Arts and Sciences (KNAW).

REFERENCES

1. **Allen, C., G. Paraskevakou, C. Liu, I. D. Iankov, P. Zollman, and E. Galanis.** 2008. Oncolytic measles virus strains in the treatment of gliomas. Expert Opin. Biol. Ther. **8:**213–220.
2. **Cattaneo, R., T. Miest, E. V. Shashkova, and M. A. Barry.** 2008. Reprogrammed viruses as cancer therapeutics: targeted, armed, and shielded. Nat. Rev. Microbiol. **6:**529–540.
3. **Cervantes-Garcia, D., R. Ortiz-Lopez, N. Mayek-Perez, and A. Rojas-Martinez.** 2008. Oncolytic virotherapy. Ann. Hepatol. **7:**34–45.
4. **Coffey, M. C., J. E. Strong, P. A. Forsyth, and P. W. Lee.** 1998. Reovirus therapy of tumors with activated Ras pathway. Science **282:**1332–1334.
5. **Csatary, L. K., G. Gosztonyi, J. Szeberenyi, Z. Fabian, V. Liszka, B. Bodey, and C. M. Csatary.** 2004. MTH-68/H oncolytic viral treatment in human high-grade gliomas. J. Neurooncol. **67:**83–93.
6. **de Haan, C. A., M. de Wit, L. Kuo, C. Montalto-Morrison, B. L. Haagmans, S. R. Weiss, P. S. Masters, and P. J. Rottier.** 2003. The glycosylation status of the murine hepatitis coronavirus M protein affects the interferogenic capacity of the virus in vitro and its ability to replicate in the liver but not the brain. Virology **312:**395–406.
7. **de Haan, C. A., P. S. Masters, X. Shen, S. Weiss, and P. J. Rottier.** 2002. The group-specific murine coronavirus genes are not essential, but their deletion, by reverse genetics, is attenuating in the natural host. Virology **296:**177–189.
8. **de Haan, C. A., L. van Genne, J. N. Stoop, H. Volders, and P. J. Rottier.** 2003. Coronaviruses as vectors: position dependence of foreign gene expression. J. Virol. **77:**11312–11323.
9. **Ekstrand, A. J., C. D. James, W. K. Cavenee, B. Seliger, R. F. Pettersson, and V. P. Collins.** 1991. Genes for epidermal growth factor receptor, transforming growth factor alpha, and epidermal growth factor and their expression in human gliomas in vivo. Cancer Res. **51:**2164–2172.
10. **Elroy-Stein, O., and B. Moss.** 1990. Cytoplasmic expression system based on constitutive synthesis of bacteriophage T7 RNA polymerase in mammalian cells. Proc. Natl. Acad. Sci. USA **87:**6743–6747.
11. **Frederick, L., X. Y. Wang, G. Eley, and C. D. James.** 2000. Diversity and frequency of epidermal growth factor receptor mutations in human glioblastomas. Cancer Res. **60:**1383–1387.

12. **Freeman, A. I., Z. Zakay-Rones, J. M. Gomori, E. Linetsky, L. Rasooly, E. Greenbaum, S. Rozenman-Yair, A. Panet, E. Libson, C. S. Irving, E. Galun, and T. Siegal.** 2006. Phase I/II trial of intravenous NDV-HUJ oncolytic virus in recurrent glioblastoma multiforme. Mol. Ther. **13:**221–228.
13. **Fuerst, T. R., E. G. Niles, F. W. Studier, and B. Moss.** 1986. Eukaryotic transient-expression system based on recombinant vaccinia virus that synthesizes bacteriophage T7 RNA polymerase. Proc. Natl. Acad. Sci. USA **83:**8122–8126.
14. **Galanis, E., R. Vile, and S. J. Russell.** 2001. Delivery systems intended for in vivo gene therapy of cancer: targeting and replication competent viral vectors. Crit. Rev. Oncol. Hematol. **38:**177–192.
15. **Gallagher, T. M.** 1997. A role for naturally occurring variation of the murine coronavirus spike protein in stabilizing association with the cellular receptor. J. Virol. **71:**3129–3137.
16. **Guo, Z. S., S. H. Thorne, and D. L. Bartlett.** 2008. Oncolytic virotherapy: molecular targets in tumor-selective replication and carrier cell-mediated delivery of oncolytic viruses. Biochim. Biophys. Acta **1785:**217–231.
17. **Jiang, H., F. McCormick, F. F. Lang, C. Gomez-Manzano, and J. Fueyo.** 2006. Oncolytic adenoviruses as antiglioma agents. Expert Rev. Anticancer Ther. **6:**697–708.
18. **Kaufmann, M., P. Lindner, A. Honegger, K. Blank, M. Tschopp, G. Capitani, A. Pluckthun, and M. G. Grutter.** 2002. Crystal structure of the anti-His tag antibody 3D5 single-chain fragment complexed to its antigen. J. Mol. Biol. **318:**135–147.
19. **Kuo, L., G. J. Godeke, M. J. Raamsman, P. S. Masters, and P. J. Rottier.** 2000. Retargeting of coronavirus by substitution of the spike glycoprotein ectodomain: crossing the host cell species barrier. J. Virol. **74:**1393–1406.
20. **Lamfers, M. L., D. Gianni, C. H. Tung, S. Idema, F. H. Schagen, J. E. Carette, P. H. Quax, V. W. Van Beusechem, W. P. Vandertop, C. M. Dirven, E. A. Chiocca, and W. R. Gerritsen.** 2005. Tissue inhibitor of metalloproteinase-3 expression from an oncolytic adenovirus inhibits matrix metalloproteinase activity in vivo without affecting antitumor efficacy in malignant glioma. Cancer Res. **65:**9398–9405.
21. **Libermann, T. A., H. R. Nusbaum, N. Razon, R. Kris, I. Lax, H. Soreq, N. Whittle, M. D. Waterfield, A. Ullrich, and J. Schlessinger.** 1985. Amplification, enhanced expression and possible rearrangement of EGF receptor gene in primary human brain tumours of glial origin. Nature **313:**144–147.
22. **Liu, T. C., and D. Kirn.** 2008. Gene therapy progress and prospects cancer: oncolytic viruses. Gene Ther. **15:**877–884.
23. **Lowe, P. N., and R. H. Skinner.** 1994. Regulation of Ras signal transduction in normal and transformed cells. Cell Signal **6:**109–123.
24. **Lun, X., D. L. Senger, T. Alain, A. Oprea, K. Parato, D. Stojdl, B. Lichty, A. Power, R. N. Johnston, M. Hamilton, I. Parney, J. C. Bell, and P. A. Forsyth.** 2006. Effects of intravenously administered recombinant vesicular stomatitis virus (VSV(deltaM51)) on multifocal and invasive gliomas. J. Natl. Cancer Inst. **98:**1546–1557.
25. **Lun, X., W. Yang, T. Alain, Z. Q. Shi, H. Muzik, J. W. Barrett, G. McFadden, J. Bell, M. G. Hamilton, D. L. Senger, and P. A. Forsyth.** 2005. Myxoma virus is a novel oncolytic virus with significant antitumor activity against experimental human gliomas. Cancer Res. **65:**9982–9990.
26. **Marcato, P., M. Shmulevitz, D. Pan, D. Stoltz, and P. W. Lee.** 2007. Ras transformation mediates reovirus oncolysis by enhancing virus uncoating, particle infectivity, and apoptosis-dependent release. Mol. Ther. **15:**1522–1530.
27. **Martuza, R. L., A. Malick, J. M. Markert, K. L. Ruffner, and D. M. Coen.** 1991. Experimental therapy of human glioma by means of a genetically engineered virus mutant. Science **252:**854–856.
28. **Miller, C. R., D. J. Buchsbaum, P. N. Reynolds, J. T. Douglas, G. Y. Gillespie, M. S. Mayo, D. Raben, and D. T. Curiel.** 1998. Differential susceptibility of primary and established human glioma cells to adenovirus infection: targeting via the epidermal growth factor receptor achieves fiber receptor-independent gene transfer. Cancer Res. **58:**5738–5748.
29. **Nakamura, T., K. W. Peng, M. Harvey, S. Greiner, I. A. Lorimer, C. D. James, and S. J. Russell.** 2005. Rescue and propagation of fully retargeted oncolytic measles viruses. Nat. Biotechnol. **23:**209–214.
30. **Nemunaitis, J., and J. Edelman.** 2002. Selectively replicating viral vectors. Cancer Gene Ther. **9:**987–1000.
31. **Nishikawa, R., X. D. Ji, R. C. Harmon, C. S. Lazar, G. N. Gill, W. K. Cavenee, and H. J. Huang.** 1994. A mutant epidermal growth factor receptor common in human glioma confers enhanced tumorigenicity. Proc. Natl. Acad. Sci. USA **91:**7727–7731.
32. **Norman, K. L., K. Hirasawa, A. D. Yang, M. A. Shields, and P. W. Lee.** 2004. Reovirus oncolysis: the Ras/RalGEF/p38 pathway dictates host cell permissiveness to reovirus infection. Proc. Natl. Acad. Sci. USA **101:**11099–11104.
33. **Ozduman, K., G. Wollmann, J. M. Piepmeier, and A. N. van den Pol.** 2008. Systemic vesicular stomatitis virus selectively destroys multifocal glioma and metastatic carcinoma in brain. J. Neurosci. **28:**1882–1893.
34. **Pedersen, N. C., J. F. Boyle, K. Floyd, A. Fudge, and J. Barker.** 1981. An enteric coronavirus infection of cats and its relationship to feline infectious peritonitis. Am. J. Vet. Res. **42:**368–377.
35. **Ring, C. J.** 2002. Cytolytic viruses as potential anti-cancer agents. J. Gen. Virol. **83:**491–502.
36. **Rottier, P. J., M. C. Horzinek, and B. A. van der Zeijst.** 1981. Viral protein synthesis in mouse hepatitis virus strain A59-infected cells: effect of tunicamycin. J. Virol. **40:**350–357.
37. **Russell, S. J., and K. W. Peng.** 2007. Viruses as anticancer drugs. Trends Pharmacol. Sci. **28:**326–333.
38. **Sarma, J. D., E. Scheen, S. H. Seo, M. Koval, and S. R. Weiss.** 2002. Enhanced green fluorescent protein expression may be used to monitor murine coronavirus spread in vitro and in the mouse central nervous system. J. Neurovirol. **8:**381–391.
39. **Sonabend, A. M., I. V. Ulasov, Y. Han, and M. S. Lesniak.** 2006. Oncolytic adenoviral therapy for glioblastoma multiforme. Neurosurg. Focus **20:**E19.
40. **Steffens, S., J. Tebbets, C. M. Kramm, D. Lindemann, A. Flake, and M. Sena-Esteves.** 2004. Transduction of human glial and neuronal tumor cells with different lentivirus vector pseudotypes. J. Neurooncol. **70:**281–288.
41. **Sugawa, N., A. J. Ekstrand, C. D. James, and V. P. Collins.** 1990. Identical splicing of aberrant epidermal growth factor receptor transcripts from amplified rearranged genes in human glioblastomas. Proc. Natl. Acad. Sci. USA **87:**8602–8606.
42. **Vennema, H., L. Heijnen, A. Zijderveld, M. C. Horzinek, and W. J. Spaan.** 1990. Intracellular transport of recombinant coronavirus spike proteins: implications for virus assembly. J. Virol. **64:**339–346.
43. **Verheije, M. H., T. Wurdinger, V. W. van Beusechem, C. A. de Haan, W. R. Gerritsen, and P. J. Rottier.** 2006. Redirecting coronavirus to a nonnative receptor through a virus-encoded targeting adapter. J. Virol. **80:**1250–1260.
44. **Waehler, R., S. J. Russell, and D. T. Curiel.** 2007. Engineering targeted viral vectors for gene therapy. Nat. Rev. Genet. **8:**573–587.
45. **Wickham, T. J.** 2003. Ligand-directed targeting of genes to the site of disease. Nat. Med. **9:**135–139.
46. **Wong, A. J., J. M. Ruppert, S. H. Bigner, C. H. Grzeschik, P. A. Humphrey, D. S. Bigner, and B. Vogelstein.** 1992. Structural alterations of the epidermal growth factor receptor gene in human gliomas. Proc. Natl. Acad. Sci. USA **89:**2965–2969.
47. **Wurdinger, T., M. H. Verheije, K. Broen, B. J. Bosch, B. J. Haijema, C. A. de Haan, V. W. van Beusechem, P. J. Rottier, and W. R. Gerritsen.** 2005. Soluble receptor-mediated targeting of mouse hepatitis coronavirus to the human epidermal growth factor receptor. J. Virol. **79:**15314–15322.
48. **Wurdinger, T., M. H. Verheije, M. Raaben, B. J. Bosch, C. A. de Haan, V. W. van Beusechem, P. J. Rottier, and W. R. Gerritsen.** 2005. Targeting non-human coronaviruses to human cancer cells using a bispecific single-chain antibody. Gene Ther. **12:**1394–1404.
49. **Yamazaki, H., Y. Ohba, N. Tamaoki, and M. Shibuya.** 1990. A deletion mutation within the ligand-binding domain is responsible for activation of epidermal growth factor receptor gene in human brain tumors. Jpn. J. Cancer Res. **81:**773–779.
50. **Yount, B., M. R. Denison, S. R. Weiss, and R. S. Baric.** 2002. Systematic assembly of a full-length infectious cDNA of mouse hepatitis virus strain A59. J. Virol. **76:**11065–11078.